journal

J. Am. Ceram. Soc., 74 [12] 2979–87 (1991)

Enhanced Fracture Toughness in Layered Microcomposites of Ce-ZrO_2 and Al_2O_3

David B. Marshall* and Joseph J. Ratto

Rockwell International Science Center, Thousand Oaks, California 91360

Fred F. Lange*

Materials Department, University of California, Santa Barbara, California 93106

Laminar composites, containing layers of Ce-ZrO_2 and either Al_2O_3 or a mixture of Al_2O_3 and Ce-ZrO_2, have been fabricated using a colloidal method that allowed formation of layers with thicknesses as small as 10 μm. Strong interactions between these layers and the martensitic transformation zones surrounding cracks and indentations have been observed. In both cases, the transformation zones spread along the region adjacent to the layer, resulting in an increased fracture toughness. The enhanced fracture toughness was observed for cracks growing parallel to the layers as well as for those that were oriented normal to the layers. [Key words: laminates, fracture toughness, cerium, zirconia, alumina.]

I. Introduction

High fracture toughnesses, in the range 10 to 14 MPa · $m^{1/2}$, have been achieved recently in ceria-partially-stabilized zirconia (Ce-TZP) that undergoes martensitic transformation from tetragonal to monoclinic phase.[1-8] However, the shapes of the transformation zones surrounding cracks in these materials are not optimal for producing large transformation toughening.[9] Whereas in other zirconia ceramics of comparable toughness (magnesia-partially-stabilized zirconia, Mg-PSZ) the transformation zone extends approximately equal distances ahead and to the side of a crack,[10] the zone in Ce-TZP is very elongated, extending ahead of the crack a distance of 10 to 20 times the zone width.[1-4] The extra transformed material ahead of the crack degrades the toughness; calculation of the crack tip shielding from zones with such shapes indicates that the increase in fracture toughness due to transformation shielding is about a factor of 2 smaller for an elongated frontal zone typical of Ce-TZP than for a semicircular frontal zone shape characteristic of Mg-PSZ.[9] Therefore, substantial benefit should result if the microstructure of Ce-TZP could be modified to change the shape of the transformation zone.

The elongated frontal zone in Ce-TZP is thought to result from autocatalytic transformation, i.e., the sequential triggering of transformation in a grain by transformation strains in adjacent grains.[5] Autocatalytic transformation also occurs in Mg-PSZ, as evidenced by the formation of well-defined shear bands within grains.[11] The microstructure of Mg-PSZ may be thought of as dual scale; the individual precipitates that transform from tetragonal to monoclinic phase are lenticular in shape (~300 nm in diameter) and are contained within grains that are larger by about 2 orders of magnitude (~50 μm in diameter).[12] Although each transformation band contains many autocatalytically transformed precipitates, the grain boundaries are effective as barriers, which arrest the propagating band. In Ce-TZP, there is no such large-scale barrier to arrest a developing transformation band; in this case, the transforming units are the individual grains and there is no larger-scale microstructural unit.

In this paper, we describe an approach for introducing a large-scale microstructural unit into Ce-TZP, in the form of layers of either Al_2O_3 or a mixture of Al_2O_3 and Ce-TZP. Based on the above discussion, the optimum separation of the layers would be expected to be a factor of ~10 to 100 times the grain size (which is ~2 μm), with individual layer thicknesses being at the lower end of the range. Layered structures satisfying this requirement have been fabricated using a colloidal method to consolidate powders. This approach has allowed formation of layers as thin as ~10 μm. Controlled crack growth experiments and indentation experiments are used to investigate the influence of these barrier layers on crack tip transformation zones and fracture toughness. The presence of the barrier layers leads to large increases in toughness and extensive *R*-curve behavior.

II. Composite Fabrication

Composites of Ce-TZP with layers of either Al_2O_3 or a mixture of 50% by volume of Al_2O_3 and Ce-ZrO_2 were fabricated using a colloidal technique. The technique involved sequential centrifuging of solutions containing suspended particles to form the layered green body, followed by drying and sintering at 1600°C for 3 h. Use was made of a technique described recently by Velamakanni *et al.*,[13] and Chang *et al.*,[14] in which an aqueous electrolyte (NH_4NO_3) was used to produce short-range repulsive hydration forces and to reduce the magnitudes of the longer-range electrostatic forces between the suspended particles. Such conditions produce a weakly attractive network of particles which prevents mass segregation during centrifugation, but, because of the lubricating action of the short-range repulsive forces, allows the particles to pack to high green density.

The relative green densities of the Al_2O_3 and Ce-ZrO_2 powders (Al_2O_3 powder from Sumitomo, Type AKP-30; Ce-ZrO_2 powder from Tosoh, Tokyo, grade TZ-12Ce) consolidated separately in this manner were approximately 60 and 50 vol%, respectively. The larger shrinkage of the Ce-ZrO_2 during subsequent sintering caused cracking in some layered composites that contained pure Al_2O_3 layers (the exceptions being some thin layers, <30 μm thick). This mismatch was minimized by using the mixed composition of 50 vol% Al_2O_3 and Ce-ZrO_2 instead of pure Al_2O_3 for most specimens.

I-W. Chen—contributing editor

Manuscript No. 196697. Received May 20, 1991; approved September 26, 1991.

Supported by the U.S. Air Force Office of Scientific Research under Contract No. F49620-89-C-0031. The colloidal science research on short-range repulsive potentials that led to the method for forming the layered structure was supported at the University of California, Santa Barbara, by the Office of Naval Research under Contract No. N00014-90-J-1141.

*Member, American Ceramic Society.

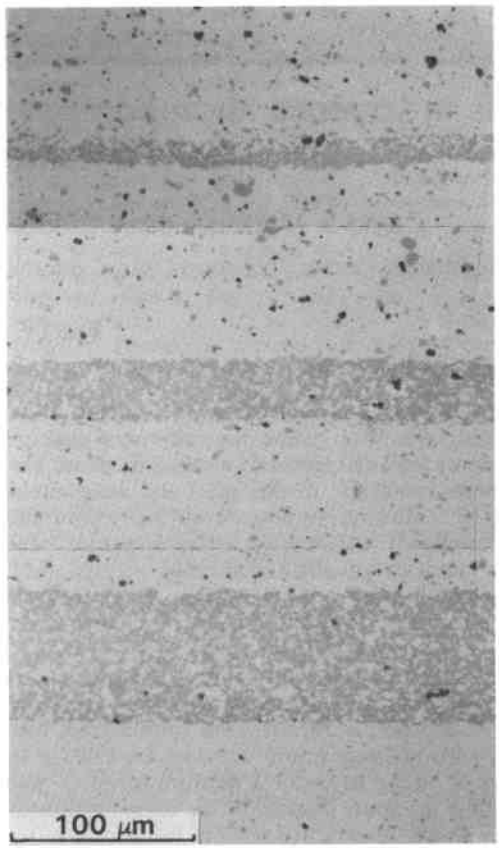

Fig. 1. Optical micrographs showing isolated layers of Al_2O_3/Ce-ZrO_2 (darker regions) with thicknesses of approximately 10, 35, and 70 μm in a matrix of Ce-TZP.

Optical micrographs of typical layers of Al_2O_3/Ce-ZrO_2 within a matrix of Ce-TZP are shown in Fig. 1. Reasonably uniform layers with thicknesses in the range 10 to 100 μm were readily formed. A multilayered structure of alternating Ce-TZP and Al_2O_3/Ce-ZrO_2 layers of thickness 35 μm is shown in Fig. 7.

III. Mechanical Properties

(1) The Role of Isolated Layers

The influence of individual layers of Al_2O_3 or 50% Al_2O_3/Ce-ZrO_2 on crack growth and transformation zones in Ce-TZP was investigated by fabricating composites containing widely spaced layers. Measurements were obtained from controlled crack growth in notched beams, fracture of smooth bars, and indentation experiments using a Vickers indenter.

Crack growth experiments with notched beams were done in two steps, using two different loading fixtures, which operated on the stage of an optical microscope and allowed high-magnification observation of the side of the beam during loading. All experiments were done in a dry nitrogen atmosphere. The dimensions of the beams were approximately 28 mm × 6 mm × 1 mm, with the initial notch of 170-μm width and approximately 2-mm depth. First, a stable crack was initiated from the root of the notch under monotonic loading, using the fixture illustrated in Fig. 2(a). The WC/Co flexure beams in series with the test specimen make the loading system extremely stiff and thereby allow stable crack growth. The beams are equivalent to very stiff springs in *parallel* with the specimen and thus act as a crack arrester, as described for different geometrical arrangements by Mai and Atkins[15] and Sakai and Inagaki.[16] This initial crack growth was induced without use of a load cell, in order to stiffen the loading system further. After thus growing the crack for ~500 μm, the loading system was changed to include a load cell with conventional four-point loading through rollers (Fig. 2(b)) in order to allow measurement of the fracture toughness (or crack growth resistance). The stress intensity factor was evaluated from the measured loads and crack lengths (obtained from optical micrographs) using the expression from Ref. 17.

Results that were obtained from a specimen containing three layers of Al_2O_3–Ce-ZrO_2 widely spaced ahead of the notch are shown in Fig. 3. After initiating stably in the immediate vicinity of the notch, the crack grew unstably when the loading system was changed to include the load cell, and arrested approximately 20 μm before the first layer of Al_2O_3/ZrO_2 (which had a thickness of ~35 μm). The width of the transformation zone over the wake of the crack, as determined by Nomarski interference, was approximately 15 μm. However, near the tip of the arrested crack, the transformation zone extended adjacent to the Al_2O_3/ZrO_3 layer for distances of more than 150 μm each side of the crack, as shown schematically in Fig. 3(b). Some transformation also occurred on the opposite side of the Al_2O_3/ZrO_2 layer, also for a distance of 150 μm both sides of the crack plane.

After further loading, the crack grew unstably through the Al_2O_3/ZrO_2 layer, into the Ce-TZP on the opposite side, and arrested again ~40 μm before the second layer (which had a thickness of 70 μm). The shape of the transformation zone

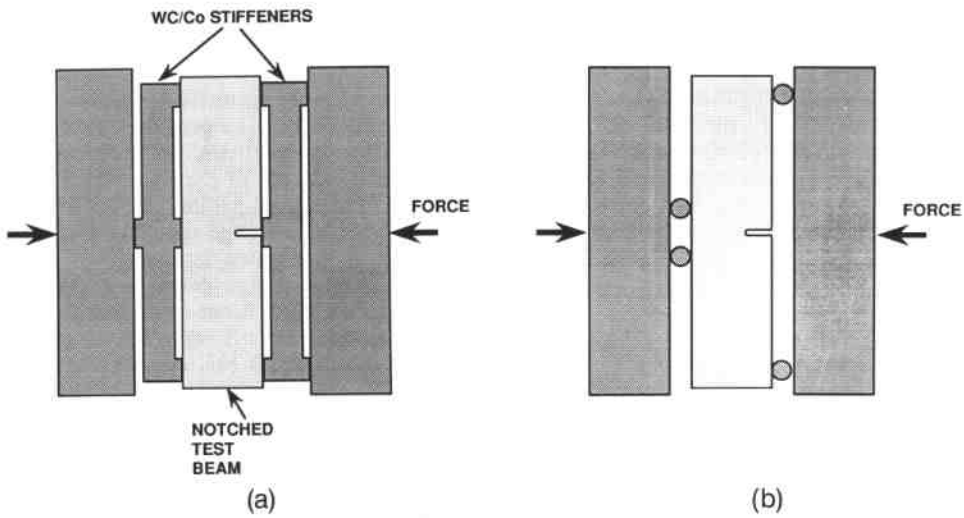

Fig. 2. Loading fixtures for notched beam fracture testing: (a) high-stiffness system used for crack initiation; (b) conventional system used for stress intensity factor measurements.

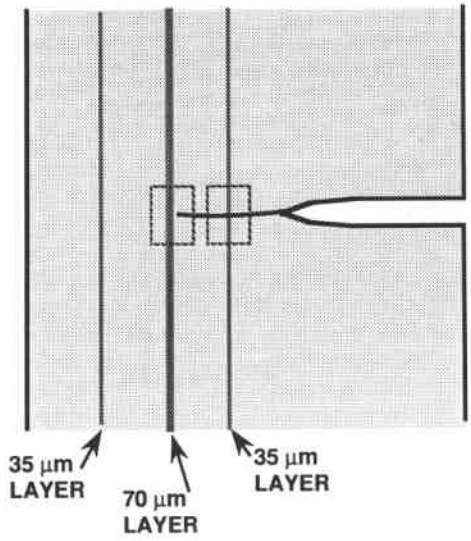

(a)

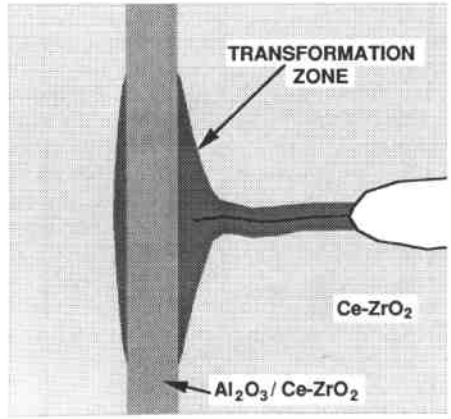

(b)

(c)

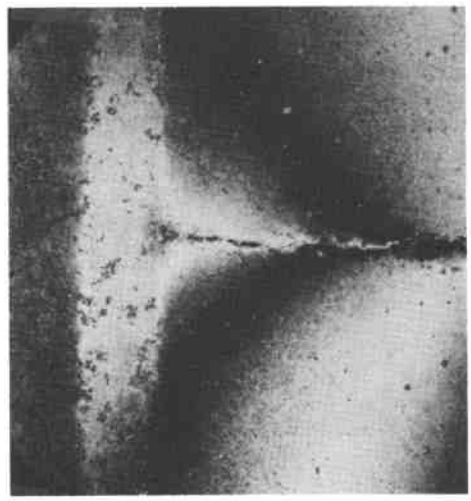

(d)

(e)

(f)

Fig. 3. Schematic of notched beam of Ce-TZP containing three layers of Al_2O_3/Ce-ZrO_2. (b) Schematic diagram of arrested crack near Al_2O_3/Ce-ZrO_2 layer, showing shape of enlarged transformation zone adjacent to the layer. (c) Nomarski interference micrograph showing arrested crack tip near Al_2O_3/ZrO_2 layer (area indicated in (a)) with widened transformation zone adjacent to layer. (d) Two-beam interference micrograph of area in (b). Reference mirror is parallel to surface remote from crack, so that fringes represent contours of constant surface uplift (due to transformation strains). (e, f) Micrographs taken as in (c) and (d) from the region in the crack wake near the first Al_2O_3/ZrO_2 layer, as indicated in (a).

along the layer near the crack tip was similar to that at the first arrest position. Nomarski interference and two-beam interference micrographs of regions around the first and second layers, with the crack tip at this position, are shown in Figs. 3(c) to (f). These results indicate that the Al_2O_3/ZrO_2 barrier layers have a much larger effect than simply arresting the growth of a transformation zone ahead of a crack; they also promote expansion of the zone to the side of the crack, which is the location that gives rise to crack tip shielding and hence toughening.[18–20]

The applied stress intensity factors were calculated at various stages of crack growth, using the measured loads and crack lengths. The fracture toughness of the Ce-ZrO_2 matrix was ≈ 5 MPa $\cdot$ $m^{1/2}$, whereas the stress intensity factor had to be raised to ≈ 10 MPa $\cdot$ $m^{1/2}$ to drive the crack across each layer. After the crack tip passed each layer, the unstable crack growth prevented continued measurement of the stress intensity factor until the crack arrested again. However, when the crack had arrested the applied stress intensity factor had decreased to ~ 5 MPa $\cdot$ $m^{1/2}$, indicating that the toughening effect of each layer decreased as it moved further into the wake of the crack. Similar results were obtained from specimens containing layers of 100% Al_2O_3 in the same Ce-TZP matrix.

Smooth beams of the same composite as in Fig. 3 were broken in bending in the two orientations shown in Figs. 4(a) and (b). In the orientation of Fig. 4(a), which is the same as that of the notched beam, failure occurred unstably at a critical load. The polished side surfaces of the beams exhibited similar evidence for widening of the transformation zone near the Al_2O_3/ZrO_2 layers as in Figs. 3(b) to (f). Therefore, this beneficial interaction occurs for fast-moving as well as stable cracks. In the orientation of Fig. 4(b), fracture also initiated unstably from the tensile surface at a critical load. However, the crack arrested before it reached the opposite side, leaving the beam intact (Fig. 4(c)). The effectiveness of the Al_2O_3/ZrO_2 layers in arresting this crack is especially noteworthy since there were only two layers in the beam, accounting for 2% of its volume. On the surface that had been loaded in tension, there were several narrow bands of transformed material in addition to the crack that caused the sudden load drop, similar to observations in the literature.[2,5,6] However, some of the transformation bands were arrested at the Al_2O_3/ZrO_2 layers. There is also evidence that the crack itself arrested at the Al_2O_3/ZrO_2 layer before joining with a second crack to cause failure.

Vickers indentations in the Ce-TZP were surrounded by large zones of transformed material, which caused uplift of the surface adjacent to the indentations. Micrographs, obtained using both Nomarski interference and two-beam interference, of several such zones in the vicinities of Al_2O_3/ZrO_2 layers are shown in Fig. 5. At indentation loads up to 300 N, there was no cracking caused by the indentations. The presence of a nearby Al_2O_3/ZrO_2 layer within the transformation zone caused spreading of the zone in the region adjacent to the layer, in a pattern that is similar to the crack tip zone spreading of Fig. 3. There was also transformed material on the side opposite the indentation. The surface uplift, measured from the optical interference micrograph of Fig. 5(b), is plotted in

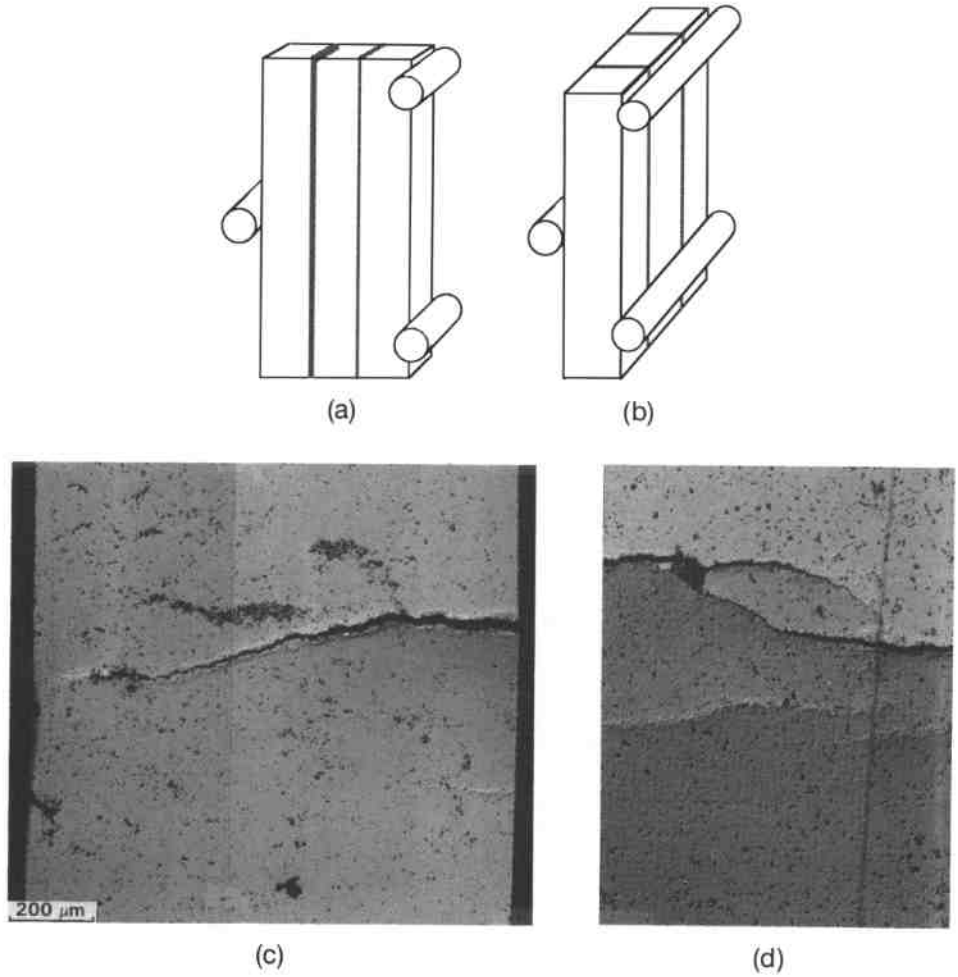

Fig. 4. (a, b) Bending test geometry showing orientations of Al_2O_3/ZrO_2 layers relative to bending direction. (c) Side view of crack in specimen oriented as in (b), showing crack arrest before complete failure. (d) Tensile surface of specimen from (c) showing crack arrest at Al_2O_3/ZrO_2 layer and arrest of transformation bands at the Al_2O_3/ZrO_2 layer (note the transformation band can also be seen on the side surface in (c)).

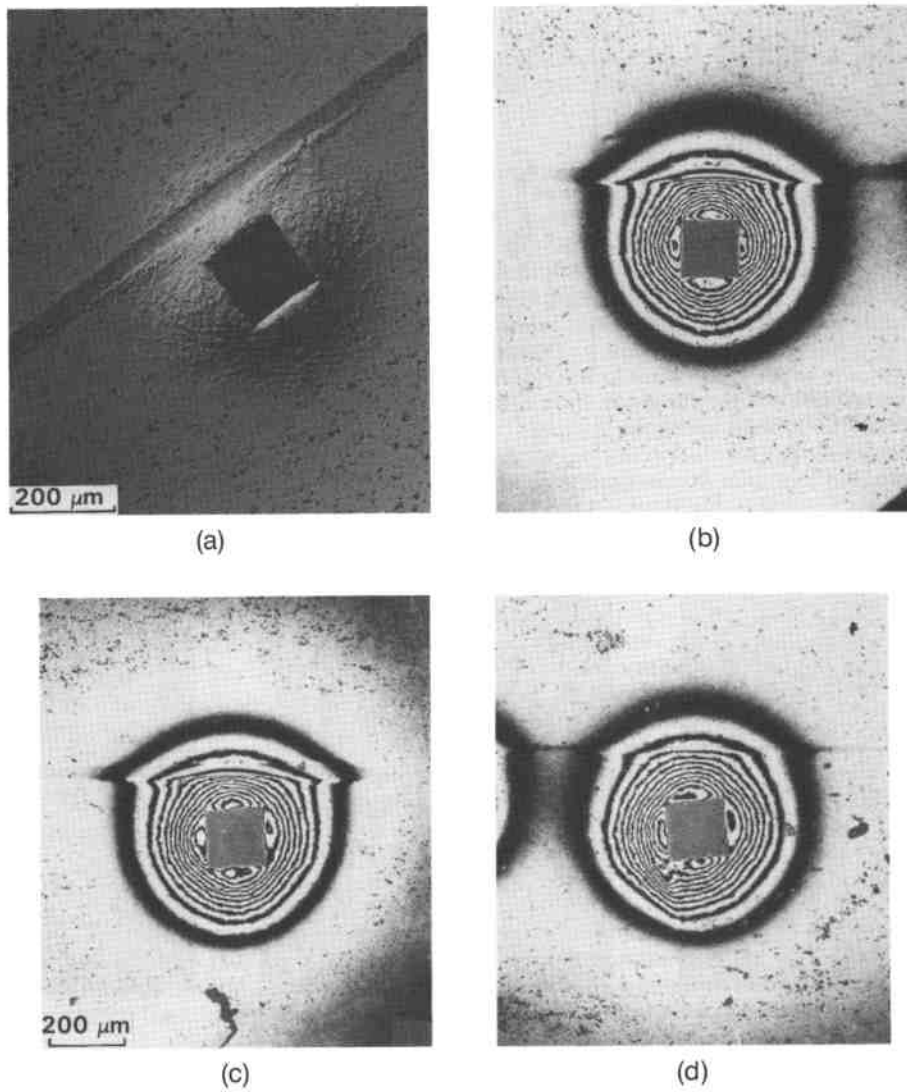

Fig. 5. Vickers indentation (200-N load) near layers of Al_2O_3 and Al_2O_3/ZrO_2 showing interaction of layers with transformation zone. (a) Nomarski interference, Al_2O_3/ZrO_2 layer 30 μm thick. (b–d) Optical interference micrographs with reference mirror parallel to specimen surface remote from indentations (fringes represent contours of surface uplift): (b) Al_2O_3/ZrO_2 layer 30 μm thick, (c) Al_2O_3 layer 30 μm thick, and (d) Al_2O_3 layer 10 μm thick.

Fig. 6 along several lines near the indentation, as depicted in the inset of Fig. 6. The presence of the Al_2O_3/ZrO_2 layer caused substantially larger uplift everywhere on the side of the indentation that is closer to the layer. The surface of the Al_2O_3/ZrO_2 layer is depressed relative to the adjacent transformed Ce-TZP material. However, this Al_2O_3/ZrO_2 layer is uplifted *more* than the Ce-TZP surface at corresponding positions on the opposite side of the indentation. This observation provides evidence that the Al_2O_3/ZrO_2 layer caused spreading of the transformation zone adjacent to the layer in the subsurface regions as well as along the surface, and/or a larger concentration of transformed material in the region adjacent to the layer.

(2) Response of Multilayered Structures

The influence of multilayered microstructures on transformation zone shapes and toughening was investigated using a specimen containing 19 layers of alternating Ce-TZP and Al_2O_3/ZrO_2, each of 35-μm thickness, in the center of a beam of Ce-TZP. An additional isolated 35-μm layer of Al_2O_3 was located ~1 mm from the multilayered region (Fig. 7(a)).

The toughening experienced by cracks oriented normal to the layers was evaluated by growing a crack in a notched beam using the loading procedure described in the previous section. The tip of the initial crack that was introduced with the stiff loading system was about halfway between the end of the notch and the first of the multiple layers (550 μm from the notch and 440 μm from the first layer). Further loading with the more compliant loading system, which allowed continuous load measurement, caused stable growth up to and

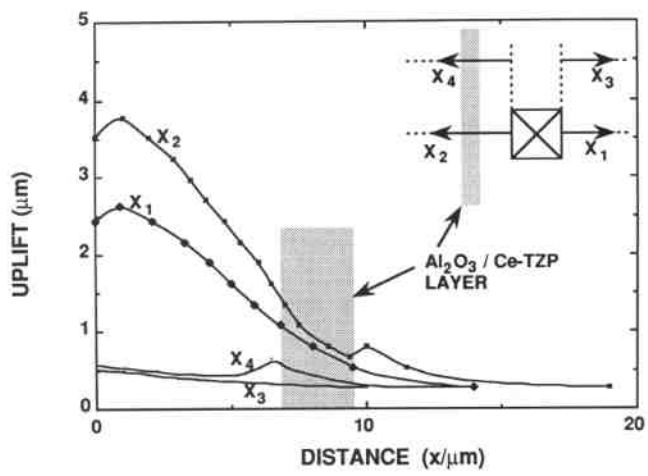

Fig. 6. Surface uplift measured from Fig. 5(b) along four paths as indicated.

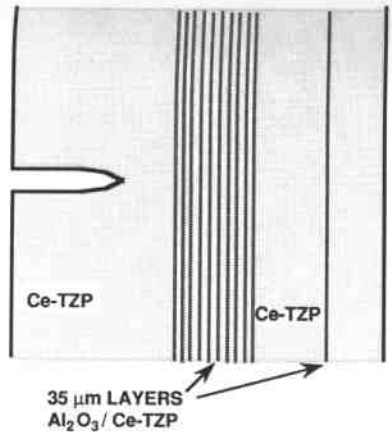

(a)

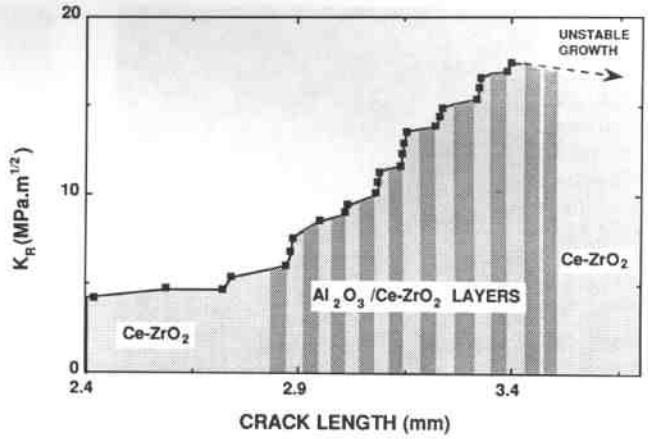

(b)

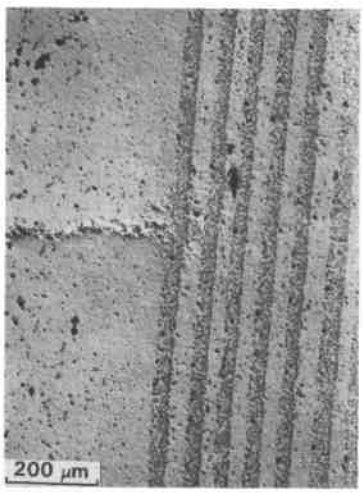

(c)

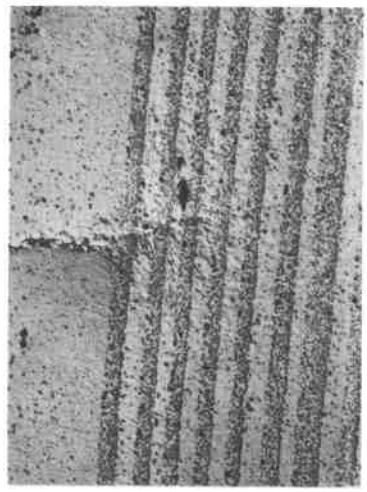

(d)

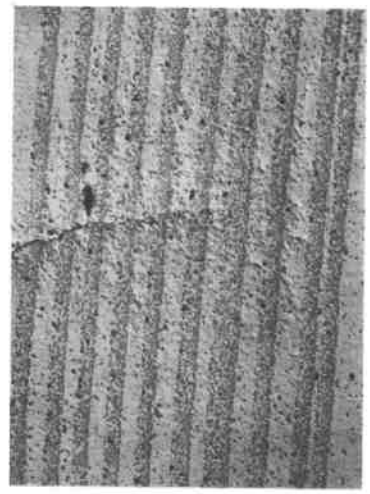

(e)

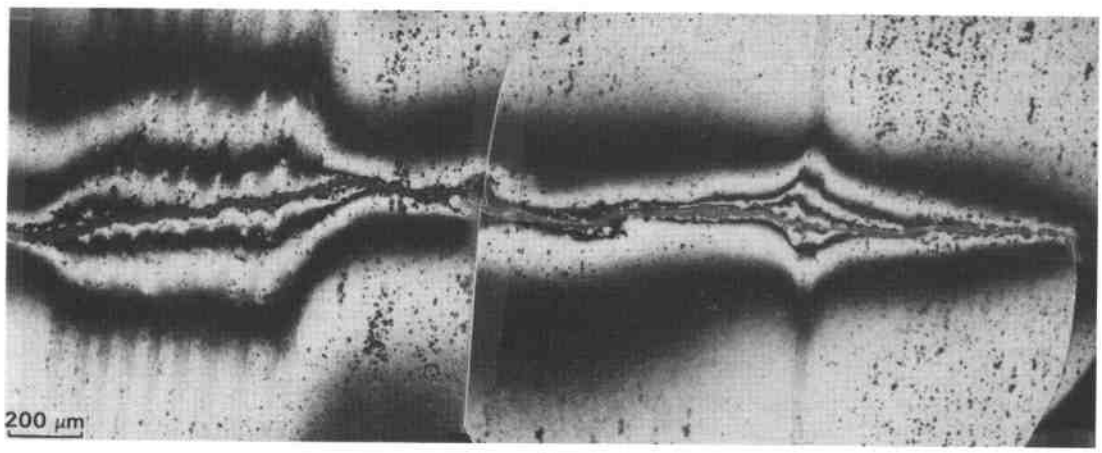

(f)

Fig. 7. (a) Multilayered region embedded within a matrix of Ce-TZP. (b) Critical applied stress intensity factor for crack growth up to and through the multilayered region of (a). (c–e) In situ optical micrographs (Nomarski interference) showing crack tip at several stages of growth through the multilayered region. (f) Optical interference micrographs of specimen in (a) to (c) after the crack had grown past the isolated layer. Reference mirror is parallel to undistorted specimen surface, so that fringes represent contours of out-of-plane surface displacements (the discontinuity in the lower central region is due to the joining of two micrographs with imperfect matching of the reference mirror positions).

through the multiple layers. However, as the crack approached the last of the layers, it extended unstably for 1.5 mm and arrested at a position 400 μm past the isolated layer.

The applied stress intensity factor, K_R, needed to extend the crack up to and through the multiple layers is shown in Fig. 7(b), and micrographs showing the crack tip at several positions within the layers are shown in Figs. 7(c) to (e). The critical stress intensity factor increased from approximately 5 MPa $\cdot$ m$^{1/2}$ in the Ce-TZP to 17.5 MPa $\cdot$ m$^{1/2}$ as the crack approached the end of the layered region. A corresponding increase in the size of the transformation zone surrounding the crack tip is evident in the micrographs of Figs. 7(c) to (e).

Surface distortions due to the volume strain associated with the transformation can be detected as far as 300 μm from the crack plane, whereas the zone width in the single phase Ce-TZP is only ~15 μm.

The increased width of the transformation zone within the layered region is more clearly evident in the optical interference micrograph of Fig. 7(f), in which the fringes represent contours of surface uplift adjacent to the crack. This micrograph was obtained after the load was removed at the conclusion of the experiment. The surface uplift adjacent to the crack is also larger (by a factor of about 2) within the layered region than in the single-phase Ce-TZP, even though the uplift is constrained by the higher-stiffness Al_2O_3/ZrO_2 layers, and the average volume fraction of the Ce-ZrO_2 is lower in the layered region. Both the zone width and the magnitude of the surface uplift adjacent to the crack decreased where the crack grew unstably out of the multilayered region into the single-phase Ce-ZrO_2, and increased again as the crack passed through the isolated Al_2O_3/ZrO_2 layer.

The response of cracks oriented parallel to the layers was assessed by loading a double cantilever beam using another fixture on the stage of the optical microscope. The cantilever beam was cut, as shown in Fig. 8(a), from a region of the specimen that contained a conveniently located large processing flaw, which served as an initial sharp crack (a flat nonsintered region ~1 mm in diameter at the edge of the multilayered area). Micrographs obtained at two stages during loading are shown in Figs. 8(b) and (c). As the load was increased initially, a zone of material within the single-phase Ce-TZP ahead and to one side of the crack tip transformed before the crack began to grow. With further load increase, the crack grew but was forced to cross the first layer of Al_2O_3/ZrO_2, presumably because of the compressive stresses due to the transformation zone on one side of the crack. The crack then grew along the first layer of Ce-ZrO_2 within the multilayered region, causing transformation in an increasingly wide zone of adjacent layers. The stress intensity factor was not evaluated during this test because the ends of the beam were glued into the loading fixture rather than being loaded through pins. Nevertheless, it is clear that the layers caused an enhancement of the width of the transformation zone, and hence the toughness, in this orientation as well as in the normal orientation.

IV. Discussion

The results in the previous section show that the presence of layers of Al_2O_3 or Al_2O_3/ZrO_2 in Ce-TZP can dramatically modify the sizes and shapes of the transformation zones around cracks. Two effects have been identified. One is the anticipated truncation of the elongated frontal zone, as discussed in the Introduction, which can increase the toughening due to crack shielding by a factor of approximately 2. The other, unexpected effect is the spreading of the transformation zones along the regions adjacent to the layers.

The zone spreading must be driven by the modification of the stress field outside the transformation zone resulting from the nontransformable nature of the layers and/or their higher elastic stiffness. Residual stress due to the difference in thermal expansion coefficients of the Ce-TZP and the Al_2O_3-containing layers could potentially influence zone spreading in multilayered composites, where, for example, the magnitude of the stress would be as high as ~100 MPa if the layer thicknesses were equal. However, in the present experiments, the zone spreading was observed around cracks and indentations near isolated layers, which represented less than 1% of the total specimen volume. In this case the residual stress in the Ce-TZP was negligibly small and therefore was not a significant influence on the spreading of the transformation zones. This conclusion is further supported by observations that layers containing 50% Al_2O_3 or 100% Al_2O_3 (for which the thermal expansion mismatches with the Ce-TZP differ) caused the same degree of zone spreading (e.g., Figs. 5(b) and (c)).

The combined effects of the zone spreading and truncation caused an increase in the fracture toughness of the layered material by a factor of 3.5 (from 5 to 17.5 MPa · $m^{1/2}$). Noting that the measured toughnesses are given by the sum of the

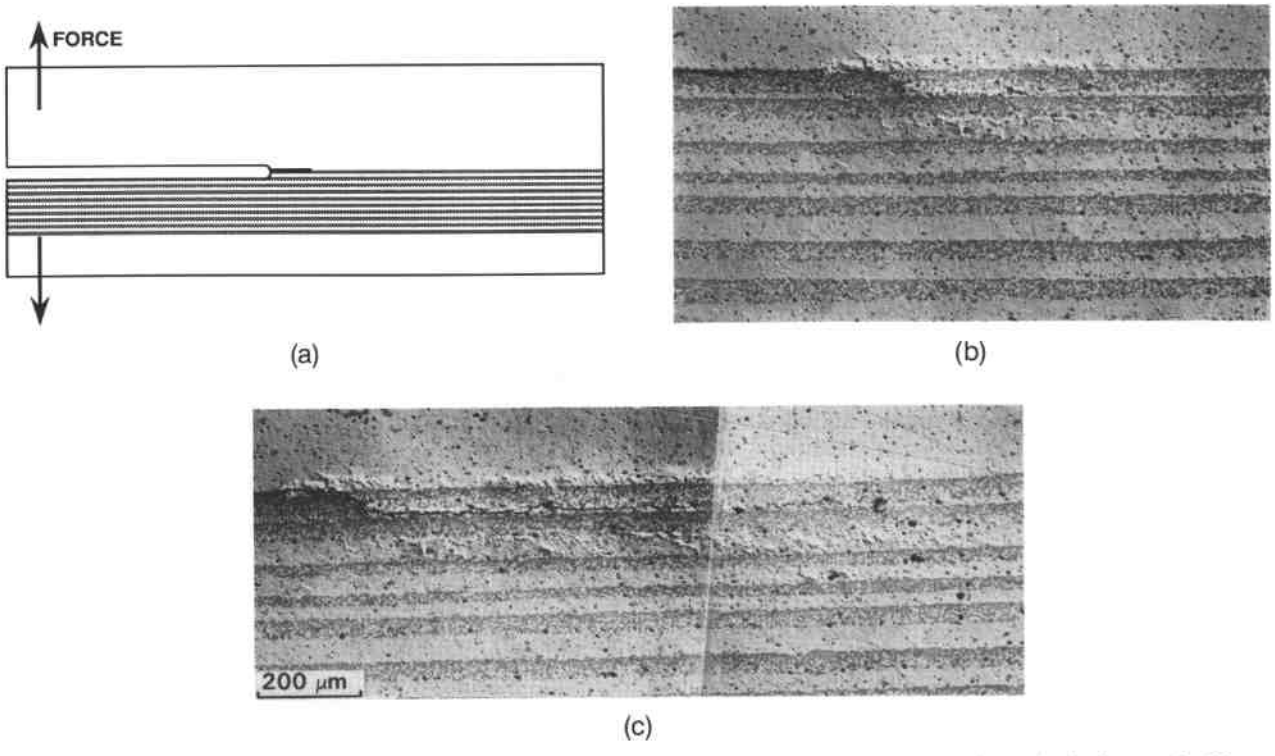

Fig. 8. (a) Schematic diagram of double cantilever beam cut from same composite as in Fig. 7. (b, c) In situ optical micrographs (Nomarski interference) showing crack and surrounding transformation zone at several stages of growth along the layers.

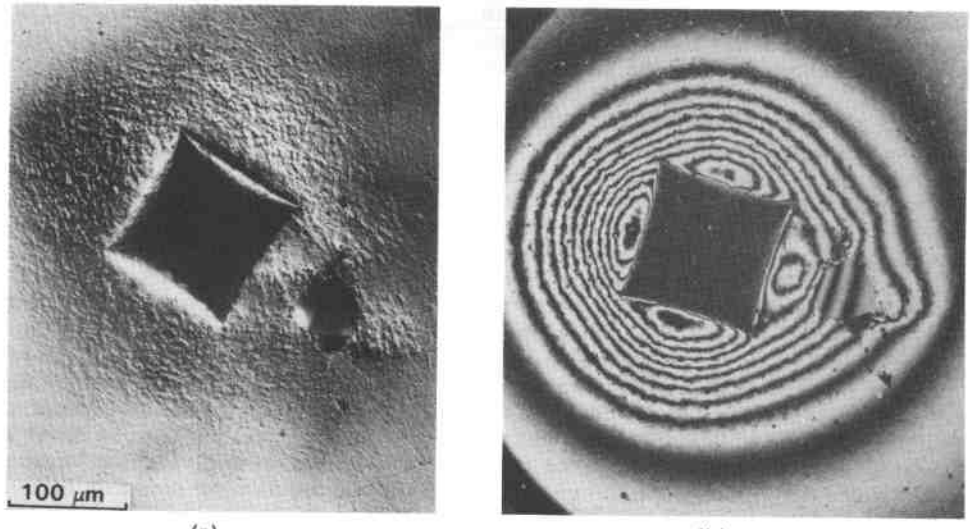

Fig. 9. Vickers indentation (200-N load) near sapphire fiber in Ce-TZP matrix, showing interaction of fiber with transformation zone: (a) Nomarski interference, (b) two-beam interference with reference mirror parallel to specimen surface remote from indentation.

intrinsic toughness of the Ce-TZP without any transformation zone and the crack tip shielding component, K_s, due to the transformation zone, the observed toughness increase corresponds to an increase in K_s by a factor of 5.

The Ce-ZrO_2 material used in this preliminary study exhibited a fracture toughness of ~5 MPa·$m^{1/2}$ and a transformation zone size of ~15 μm (Figs. 7(b) and (c)). These values are substantially smaller than the toughnesses and zone sizes reported in more transformable Ce-ZrO_2 materials[1-8] ($K_R \approx$ 14 MPa·$m^{1/2}$ and zone sizes of several hundred micrometers). However, despite this relatively low starting toughness, the multilayered microstructure was characterized by a crack resistance curve that went as high as 17.5 MPa·$m^{1/2}$, and which had not begun to saturate to a steady-state value when the crack encountered the end of the layered microstructure. This peak value of K_R is one of the highest toughnesses recorded in a ceramic material, being surpassed only by weakly bonded fiber-reinforced composites,[21] weakly bonded laminar composites,[22] and by some Mg-PSZ materials immediately after heat treatment[23,24] (the high-toughness Mg-PSZ materials age and lose some of their toughening at room temperature). There is clearly a potential for substantially higher fracture toughnesses in layered microstructures fabricated with the higher-toughness Ce-TZP starting materials. Fabrication of such materials is under way.

The mechanisms of toughening enhancement observed here should not be restricted to the laminar geometry used in this study. Similar effects may be expected for any high-modulus, nontransforming microstructural unit, such as continuous or chopped fibers or platelets, distributed over a similar spatial scale as the layers. An example of the interaction of a transformation zone around an indentation with an isolated sapphire fiber in the Ce-TZP matrix is shown in Fig. 9. By direct analogy with the effect of the Al_2O_3 layers, the sapphire fiber caused spreading of the transformation zone and a larger overall surface uplift in the vicinity of the fiber.

V. Conclusions

Laminar composites containing alternating layers of Ce-TZP and a mixture of Al_2O_3 and Ce-ZrO_2 have been fabricated using a colloidal technique. In situ observations during controlled crack growth experiments in these microcomposites have yielded the following results:

(1) The layers interacted strongly with the transformation zones surrounding cracks and indentations, causing the zones to spread along the regions adjacent to the layers and leading to enhanced fracture toughness.

(2) Multilayered microstructures exhibited *R*-curve behavior for cracks oriented normal to the layers, with the critical stress intensity factor increasing by a factor of 3.5 from the starting toughness of the Ce-TZP (~5 MPa·$m^{1/2}$) to a value of at least 17.5 MPa·$m^{1/2}$. (This peak value had not saturated to a steady state, but instead was limited by the crack having reached the end of the multilayered region.)

(3) Zone spreading and toughening effects were observed for cracks growing parallel to the layers as well as for those oriented normal to the layers.

References

[1]M.V. Swain, R.H.J. Hannink, and J. Drennan, "Some Interfacial Related Properties of Transformation Toughened Ceramics"; p. 819 in *Ceramic Microstructures '86, Role of Interfaces*. Edited by J.A. Pask and A.G. Evans. Plenum, New York, 1987.

[2]R.H.J. Hannink and M.V. Swain, "Metastability of Martensitic Transformation in a 12 mol% Ceria–Zirconia Alloy: Deformation and Fracture Observations," *J. Am. Ceram. Soc.*, **72** [1] 90–98 (1989).

[3]L.R.F. Rose and M.V. Swain, "Transformation Zone Shape in Ceria-Partially-Stabilized Zirconia," *Acta Metall.*, **36** [4] 955–62 (1988).

[4]C.-S. Yu and D.K. Shetty, "Transformation Zone Shape, Size, and Crack-Growth-Resistance (*R*-Curve) Behavior of Ceria-Partially-Stabilized Zirconia Polycrystals," *J. Am. Ceram. Soc.*, **72** [6] 921–28 (1989).

[5]P.E. Reyes-Morel and I-W. Chen, "Transformation Plasticity of CeO_2-Stabilized Tetragonal Zirconia Polycrystals: I, Stress Assistance and Autocatalysis," *J. Am. Ceram. Soc.*, **72** [5] 343–53 (1988).

[6]P.E. Reyes-Morel, J.-S. Cherng, and I-W. Chen, "Transformation Plasticity of CeO_2-Stabilized Tetragonal Zirconia Polycrystals: II, Pseudoelasticity and Shape Memory Effects," *J. Am. Ceram. Soc.*, **71** [8] 648–57 (1988).

[7]K.E. Tsukuma and M. Shimada, "Strength, Fracture Toughness, and Vickers Hardness of CeO_2-Stabilized Tetragonal Zirconia Polycrystals (Ce-TZP)," *J. Mater. Sci.*, **204** [4] 1178–84 (1985).

[8]T. Sato, T. Endo, and M. Shimada, "Postsintering Hot Isostatic Pressing of Ceria-Doped Tetragonal Zirconia/Alumina Composites in an Argon–Oxygen Gas Atmosphere," *J. Am. Ceram. Soc.*, **72** [5] 761–64 (1989).

[9]D.B. Marshall, "Crack Shielding in Ceria-Partially-Stabilized Zirconia," *J. Am. Ceram. Soc.*, **73** [10] 3119–21 (1990).

[10]D.B. Marshall, M.C. Shaw, R.H. Dauskardt, R.O. Ritchie, M. Readey, and A.H. Heuer, "Crack Tip Transformation Zones in Toughened Zirconia," *J. Am. Ceram. Soc.*, **73** [9] 2659–66 (1990).

[11]A.H. Heuer, M. Rühle, and D.B. Marshall, "On the Thermoelastic Transformation in Tetragonal ZrO_2," *J. Am. Ceram. Soc.*, **73** [4] 1084–93 (1990).

[12]R.H.J. Hannink and M.V. Swain, "Magnesia-Partially-Stabilized Zirconia: The Influence of Heat Treatment on Thermomechanical Properties," *J. Aust. Ceram. Soc.*, **18** [2] 53–62 (1982).

[13]B.V. Velamakanni, J.C. Chang, F.F. Lange, and D.S. Pearson, "New Method for Efficient Colloidal Particle Packing via Modulation of Repulsive Lubricating Hydration Forces," *Langmuir*, **6**, 1323–25 (1990).

[14]J.C. Chang, B.V. Velamakanni, F.F. Lange, and D.S. Pearson, "Centrifugal Consolidation of Al_2O_3 and Al_2O_3/ZrO_2 Composite Slurries vs

Interparticle Potentials: Particle Packing and Mass Segregation," *J. Am. Ceram. Soc.*, **74** [9] 2201–204 (1991).

[15]Y.W. Mai and A.G. Atkins, "Crack Stability in Fracture Toughness Testing," *J. Strain Anal.*, **15** [2] 63–74 (1980).

[16]M. Sakai and M. Inagaki, "Dimensionless Load–Displacement Relation and Its Application to Crack Propagation Problems," *J. Am. Ceram. Soc.*, **72** [3] 388–94 (1989).

[17]H. Tada, *The Stress Analysis of Cracks Handbook*, 2nd ed. Paris Productions Inc., St. Louis, MO, 1985.

[18]R.M. McMeeking and A.G. Evans, "Mechanics of Transformation Toughening in Brittle Materials," *J. Am. Ceram. Soc.*, **65** [5] 242–46 (1982).

[19]D.B. Marshall, A.G. Evans, and M. Drory, "Transformation Toughening in Ceramics"; p. 289 in *Fracture Mechanics and Ceramics*, Vol. 6. Edited by R.C. Bradt, A.G. Evans, D.P.H. Hasselman, and F.F. Lange. Plenum Press, New York, 1983.

[20]A.G. Evans and R.M. Cannon, "Toughening of Brittle Solids by Martensitic Transformations," *Acta Metall.*, **34** [5] 651–800 (1986).

[21]A.G. Evans and D.B. Marshall, "The Mechanical Behavior of Ceramic Matrix Composites," *Acta Metall.*, **37** [10] 2607–83 (1989).

[22]W.J. Clegg, K. Kendall, N. McN. Alford, T.W. Button, and J.D. Birchall, "A Simple Way to Make Tough Ceramics," *Nature (London)*, **347**, 455–57 (1990).

[23]A.H. Heuer, M.J. Readey, and R. Steinbrech, "Resistance Curve Behavior of Supertough MgO-Partially-Stabilized ZrO_2," *Mater. Sci. Eng.*, **A105/106**, 83–89 (1988).

[24]M.J. Readey and A.H. Heuer, "Annealing of Test Specimens of High-Toughness Magnesia-Partially-Stabilized Zirconia," *J. Am. Ceram. Soc.*, **71** [1] C-2–C-6 (1988). □